TECHNICAL REPORT, CB No. 331

Analysis of $\eta\eta\pi^0$, 600–1350 MeV/c

D.V. Bugg, QMWC, London

June 10, 1998

Abstract

Data are presented on $\bar{p}p \to \eta\eta\pi^0$ at beam momenta of 600, 900, 1050, 1200 and 1350 MeV/c. At the central three momenta, a signal is clearly visible due to $\bar{p}p \to f_0(1770)\pi^0$, $f_0(1770) \to \eta\eta$. It has mass 1770 ± 12 MeV and width 220 ± 40 MeV, where errors cover systematic uncertainties as well as statistics.

1 Data Processing

This was identical to $\eta\eta\pi^0$ at higher momenta, so you are referred to that Technical Report. Table 1 shows numbers of events, Monte Carlo statistics and background levels estimated from the Monte Carlo simulation of all channels. There are fewer events at 600 MeV/c than at other momenta because most of the data were taken without Tony's box.

Momentum (MeV/c)	Events	Monte Carlo	Background(%)
600	2922	11753	2.8
900	9023	45923	3.9
1050	6607	22620	3.3
1200	9594	44434	3.7
1350	4648	17816	4.2

Table 1
Numbers of events, Monte Carlo and estimated background levels.

2 Features of the Data

Dalitz plots and projections on to $M_{\eta\eta}$ and $M_{\eta\pi}$ are shown in Figs. 1–5. The figures also show fitted Dalitz plots from the amplitude analysis which follows. Histograms on the projections are from the fit.

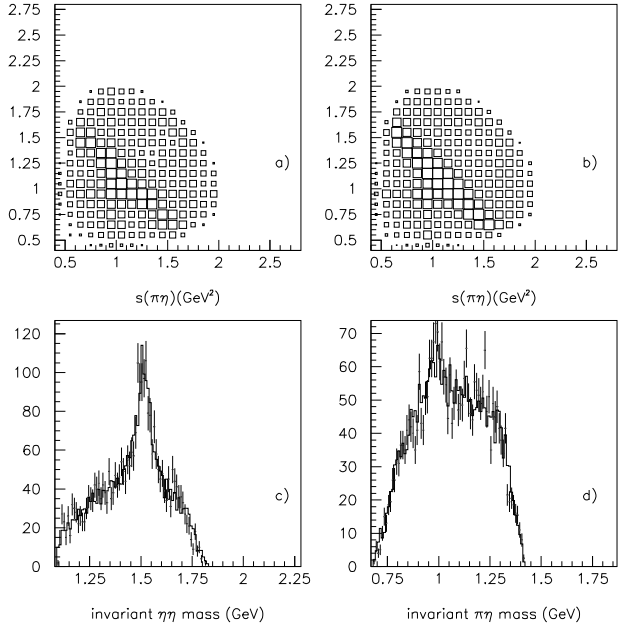

Fig.1. Dalitz plots at 600 MeV/c, (a) data, (b) fit; projection on to (c) $M(\eta\eta)$ and (d) $M(\eta\pi)$.

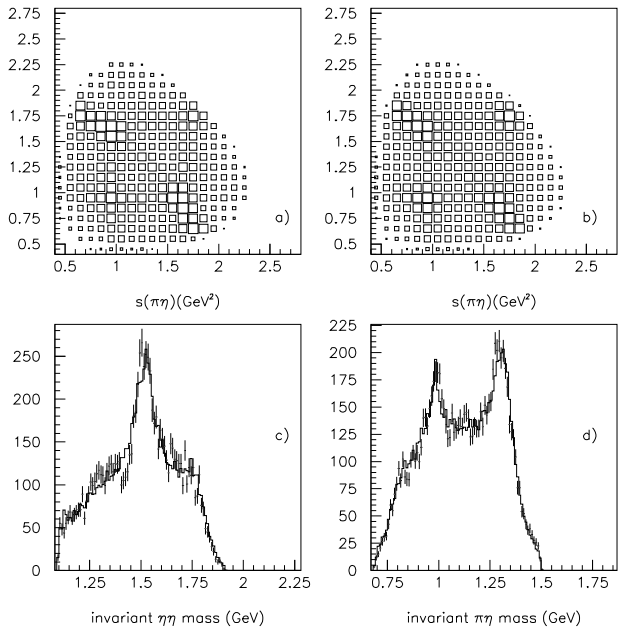

Fig 2. As Fig. 1 at 900 MeV/c

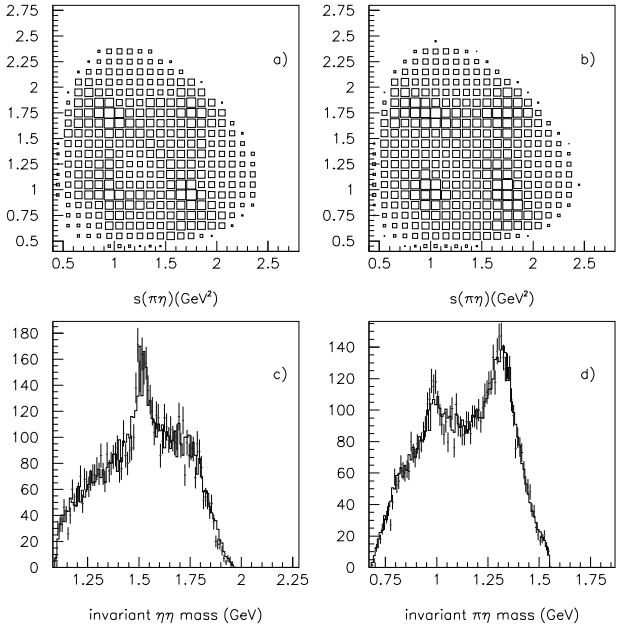

Fig 3. As Fig. 1 at 1050 MeV/c

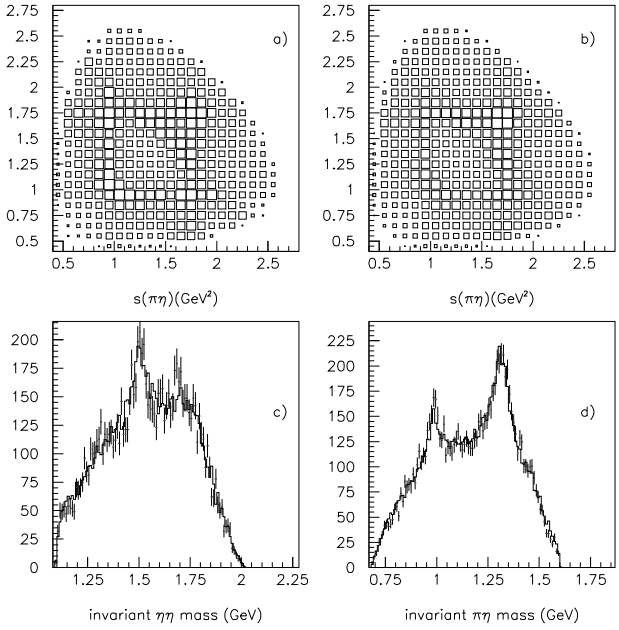

Fig 4. As Fig. 1 at 1200 MeV/c

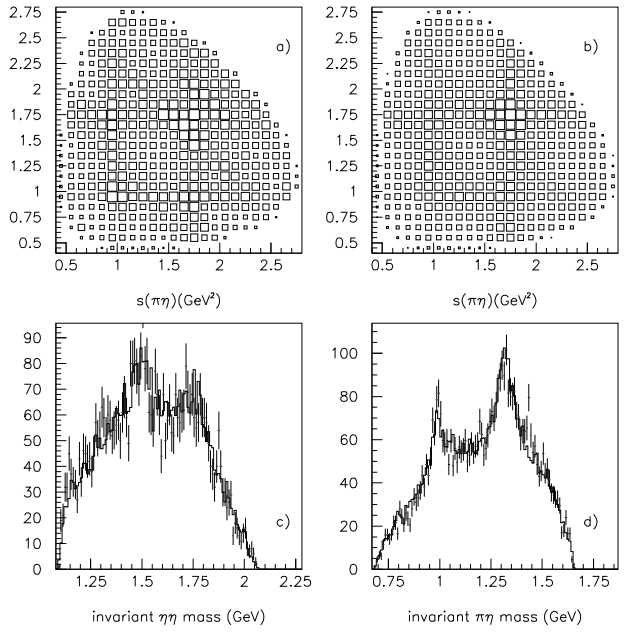

Fig 5. As Fig. 1 at 1350 MeV/c

Conspicuous features of the data are $f_0(1500)$ (diagonal bands on the Dalitz plots), $a_2(1320)$ and $a_0(980)$. However, the feature of interest is the shoulder visible in $\eta\eta$ at 1770 MeV at beam momenta from 900 to 1350 MeV/c. The amplitude analysis reveals a clear $f_0(1770)$ at 900, 1050 and 1200 MeV/c. Data at 1350 MeV/c give a small optimum at the same mass, but this result is less significant than at lower momenta.

I have searched for the $f_J(1710)$ but found no significant evidence for its presence, either with spin 0 or spin 2.

3 Amplitude Analysis

A partial wave analysis has been made of the full process of production and decay. The amplitudes included in the analysis are shown in Table 2. Amplitudes are calculated using the method of Wick rotations, explained in many previous reports. The last column of Table 2 shows the centre of mass momentum for each channel on resonance at a beam momentum of 1350 MeV/c. A rule of thumb from earlier analyses is that about 250 MeV/c is needed per unit of orbital angular momentum in the production process. That empirical rule seems to work well here. For $a_0(980)\eta$ and $a_2(1320)\pi$, $L = 3$ is required, but in neither case is there any sign of $L = 4$. That is in accord with the fact

that 4^- is not expected in the quark model until a mass of ~ 2350 MeV, i.e. a beam momentum of 1800 MeV/c.

A technicality is that it is convenient to fit 2^+ initial states with helicity $m = 0$ and 1 as basis states rather than $^3P_2$ and $^3F_2$; they are linearly related. The reason for this choice is that two $m = 1$ amplitudes turn out to be negligible.

Channel	Partial Waves	CM Momentum (MeV/c)
$a_0(980)\eta$	$^1S_0$,$^3P_1$,$^1D_2$,$^3F_3$	777
$f_0(1500)\pi$	$^1S_0$,$^3P_1$,$^1D_2$,$^3F_3$	578
$a_2(1320)\eta$	$^1D_2(L = 0 \text{ and } 2)$, $^1S_0(L = 2)$ $^3P_1, 2^+(m = 0 \text{ and } 1)$,$^3F_3(L = 1)$ $2^+(L = 3, m = 0)$	546
$f_0(1750)\pi$	$^1S_0$,$^3P_1$	386
$f_2(1270)\pi$	$^1D_2$	726
$f_2'(1525)\pi$	$^1D_2$, $^3P_1$	556
$f_2(1980)\pi$	$^1D_2$, $^3P_1$, $2^+(m = 0 \text{ and } 1)$, $^3F_3$	163

Table 2
Partial waves included in the analysis; the third column shows the centre of mass momentum on resonance for the highest beam momentum of 1350 MeV/c.

A word of warning is that, with the available statistics, there are sizable errors on the magnitudes and phases of each partial wave. For amplitudes with 8% branching fraction, errors are about $\pm 25\%$, increasing to $\pm 50\%$ for 2% branching fraction. Consequently we shall not be able to draw strong conclusions about individual partial waves. Tables of results will be given for completeness. Most partial waves follow within these sizable errors a fairly smooth dependence on centre of mass momentum. I have found that restrictions on partial waves (e.g. fixing them in magnitude or phase) have little effect on the evidence for $f_0(1770)$. Bing Song Zou is reporting data on $\bar{p}p \to \eta\pi^0\pi^0$ with roughly a factor 12-16 higher statistics. There, many resonances are visible, but phase variations with momentum are mostly small, i.e. resonances are phase coherent. In present data, phase variations are again small, although there are fluctuations of typically $\pm(10-25)^\circ$ from one momentum to another.

A technical point is that the amplitude analysis produces a fit in roughly 60 seconds of computing. This is sufficiently fast that I have been able to examine a large number (> 1500) of trials with varying ingredients in order to study the systematics of the fit, its stability and the sensitivity to every channel. Although some ambiguities are present at individual momenta (particularly

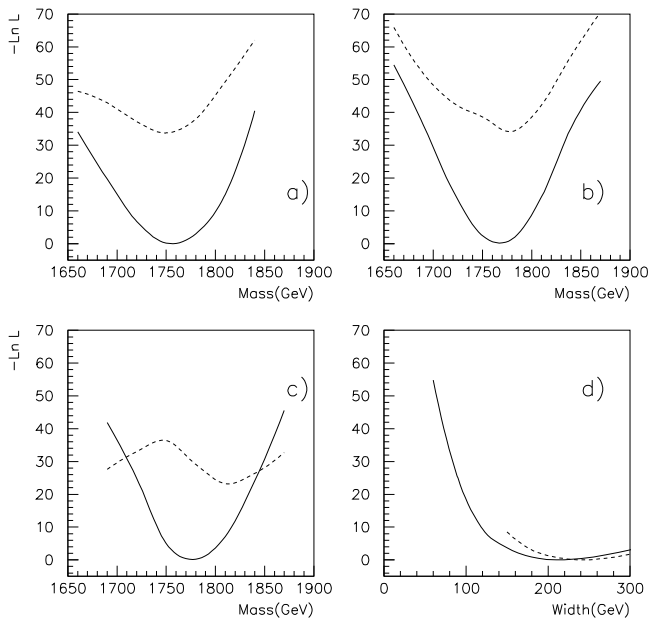

Fig. 6. Variations of log likelihood with the mass of $f_0(1770)$, full line $J = 0$, dashed line $J = 2$, (a) at 900 MeV/c, (b) at 1050 MeV/c, (c) at 1200 MeV/c; (d) the variation of log likelihood with width at 1050 MeV/c (full curve) and 1200 MeV/c (dashed).

beween $L = 0$ and $L = 2$ and between $L = 1$ and $L = 3$), I have located only one solution having a smooth variation of magnitude, and particularly phase, with momentum.

4 Evidence for $f_0(1770)$

This resonance show up most clearly at 1050 MeV/c. A scan of the mass and width immediately reveals a deep minimum for $J = 0$ with a mass of 1770 MeV; this scan is shown as the full curve on Fig. 6(b). Scans at 900 and 1200 MeV/c reveal similar optima, as shown on Figs. 6(a) and (c).

The actual optima are at $M = 1758 \pm 10$ MeV at 900 MeV/c, $M = 1770 \pm 8$ MeV at 1050 MeV/c and $M = 1775 \pm 8$ MeV at 1200 MeV/c, leading to a weighted average of $M = 1770 \pm 7$ MeV. To cover the observed variations, I assign a systematic error on the mass of ± 12 MeV. At 1350 MeV/c, the optimum is weaker, but still it optimises at $M = 1780$ MeV; that optimum is too weak to be of much significance. At 1525 MeV/c the resonance disappears. But at 1642 MeV/c it is again visible to the amplitude analysis, as shown in

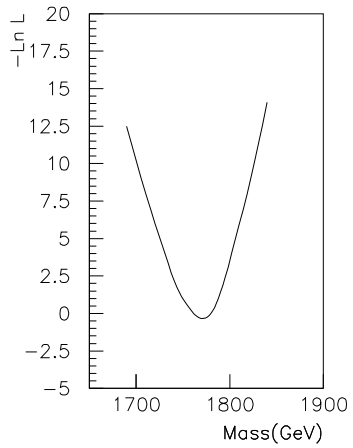

Fig. 7. Variation of log likelihood with the mass of $f_0(1770)$ for data at 1642 MeV/c.

Fig. 7. It optimises at 1775 MeV.

Fig. 6(d) shows log likelihood v. the width of $f_0(1770)$. At 1050 MeV/c, $\Gamma = 210 \pm 26$ MeV and at 1200 MeV/c, $\Gamma = 240 \pm 40$ MeV. The weighted mean is 220 MeV with a systematic error I assess as ± 40 MeV.

For momenta other than 1050 and 1200 MeV/c, there is no real optimum for the width. The curve of log likelihood v. width simply flattens out above 220 MeV.

The first column of Table 3 shows changes in log likelihood when $f_0(1770)$ is removed from the fits.

Momentum (MeV/c)	(a)	(b)	(c)	(d)
900	-81.4	-33.8	15.6	3.5
1050	-101.6	-34.2	20.3	5.8
1200	-83.0	-28.9	17.3	3.2

Table 3
Changes to log likelihood of the basic fit, (a) dropping $f_0(1770)$, (b) replacing $f_0(1770)$ by $f_2(1770)$, (c) adding $f_2(1697)$, or (d) adding $f_0(1697)$.

5 Is $\theta(1710)$ present?

If there were a second weak 0^+ resonance present at 1690–1710 MeV, it would probably be hard to separate from $f_0(1770)$. I have scanned for it, adding $^1S_0$ and $^3P_1$ amplitudes to the reference fit which includes $f_0(1770)$; but I have found nothing. Column (d) of Table 3 shows the very small improvements in log likelihood it produces for PDG values of mass and width.

So my attention has been concentrated on looking for an f_2. Here the difficulty lies in separating it from the broad $f_2(1980)$ which was located in the $\eta\eta\pi^0$ data from 1350 to 1800 MeV/c. At those momenta, it was very clear that a broad 2^+ signal peaks towards 2 GeV rather than around 1710 MeV. It is very broad, $\Gamma \sim 500$ MeV. At 1200 MeV/c, some 2^+ signal is again definitely required, but is spread over a broad mass range and is not concentrated around 1700 MeV. At lower beam momenta, confusion between $f_2(1980)$ and $f_2(1710)$ is possible, because of the limited phase space.

If I include in the amplitude analysis an f_2 of width 220 MeV instead of $f_0(1770)$, results are shown by the dashed curves of Figs. 6(a)–(c). Spin 0 gives much the better log likelihood and a better defined minimum. In making these scans, I have assumed either $J = 0$ or $J = 2$ resonances are produced with both $L = 0$ and 1 in the production channel. For $J = 0$ this implies partial waves $^1S_0$ and $^3P_1$. The former dominates completely and contributions from $^3P_1$ are barely significant. For $J = 2$, the partial waves are $^1D_2$, $^3P_1$, $^3P_2$, $^3F_2$ and $^3F_3$. Even if one disregards the fact that there are 6 more parameters for spin 2, then spin 0 is preferred at the three momenta by over 8 standard deviations.

For $J = 2$, the dashed curves show signs of optimising at the same mass as $J = 0$. This is a familiar type of phenomenon from the analysis of $4\pi^0$ data. I have shown that it is due to cross-talk between the two spins. The detector has 12° holes for entrance and exit of the beam, and these holes give rise to significant lack of orthogonality between the two possibilities.

This has been demonstrated by the following simulation. The data have first been fitted with $f_0(1770)$ and all the other amplitudes of Table 2. Then Monte Carlo events have been weighted by cross sections from this fit in order to produce simulated data sets of known content. The precise way in which this works is as follows. Events are chosen from the Monte Carlo data set using a weight w proportional to $d\sigma/d\Omega$. I define a 'cumulative' quantity Q, whose initial value is chosen at random up to a value B. Then, as each Monte Carlo event is read by the programme, the weight w is added to Q. Events with large cross section move Q forward by a large amount, and conversely events with small cross section move it forwards rather little. If Q moves past the

barrier B, the event is accepted and Q is reduced to $(Q - B)$. Usually this new value is below B, but occasionally it is still above. In that case, the event is counted twice, and so on. The value of B is chosen so that the generated data sample contains an equal number of events to real data. I have formed 10 simulated data sets in this way, starting with random Q values. It is evident that there are some correlations between them.

They have then been fitted using spin 2 instead of spin 0 for $f_J(1770)$. The average of the 10 simulations reproduces well the dashed curves of Figs. 6(a)–(c) (within the scatter of the 10 fits). In particular, the difference in log likelihood between $J = 0$ and $J = 2$ is well reproduced: $\Delta(\text{log likelihood}) \simeq 35$. These differences in log likelihood for data are shown in column (b) of Table 3. My conclusion is that this simulation shows that the minima in Figs. 6(a)–(c) for spin 2 are simply due to feed-through from spin 0. If BOTH $f_2(1770)$ and $f_0(1770)$ are included in the fit, over 90% of the signal fits as spin 0.

Could there be some additional $f_2(1697)$ present? An inspection of the $\eta\eta$ mass projection of Fig. 2 (900 MeV/c) reveals some excess of events above the fit between 1600 and 1700 MeV. In the corresponding projection of Fig. 4 (1200 MeV/c), one sees four high points immediately below 1700 MeV.

I have examined these discrepancies by adding $f_J(1697)$ to the fit using the PDG width of 175 MeV. Improvements in log likelihood are listed in columns (c) and (d) of Table 3. However, there is almost no visible improvement in the fit to mass projections in either case.

It IS possible to fit the four high bins at 1200 MeV/c using an $f_2(1690)$ with a width of $\leq$ 40 MeV; the optimum width is 25 MeV. The resulting fit is shown in Fig. 8. However, such a narrow width seems highly suspicious. In my opinion, evidence for the presence of such a narrow resonance needs to be stronger than this.

For spin 2, the improvement in log likelihood is $\sim$ 20. This appears to be greater than the improvement of 5 one expects from statistics alone. However, in no case is there an optimum at 1700 MeV. At 900 MeV/c, there is a weak optimum ($\sim$ 5 in log likelihood) at 1650 MeV. At 1050 MeV/c, there is no optimum but a slight improvement as $M \to 1800$ MeV. At 1200 MeV/c, there is a weak optimum at 1750 MeV. From past experience with $f_J(2100)$, I know that partial waves $^1D_2$, $^3P_1$, $^3P_2$, $^3F_2$ and $^3F_3$ are able to simulate accurately the flat decay angular distribution of a spin 0 resonance produced from $^1S_0$. To test this, I have tried fitting fake 2^+ signals to the simulated data sets I described above. In this case, we know the simulated data set does NOT contain 2^+. Nonetheless, I have found that the addition of an $f_2(1697)$ with $\Gamma = 175$ MeV to the fit improves log likelihood by 17 ± 3. This value agrees well with the improvements observed for real data. My conclusion is that there

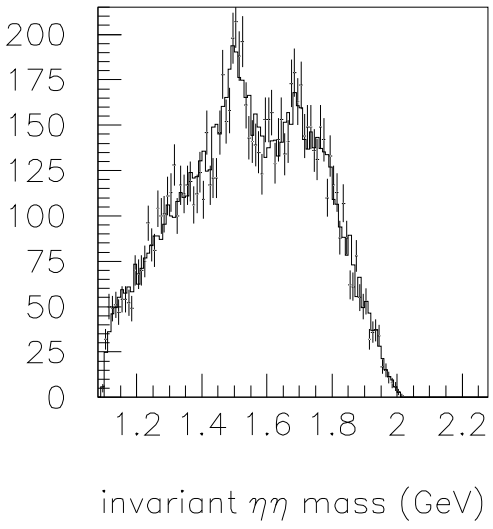

Fig. 8. The fit at 1200 MeV/c including $f_2(1690)$ with $\Gamma = 25$ MeV.

is no significant evidence for the presence of $f_J(1710)$, a disappointing result. An upper limit to the branching ratio of $f_2(1697)$ with PDG width is $\sim 4\%$ at the 90% confidence level.

6 Angular Distributions

Figs. 9-13 (displaced by TeX to the end of this report) show production angular distributions for bands centred on $a_0(980)$, $a_2(1320)$, $f_0(1500)$ and for the 1640-1840 MeV mass range. Each of the first three bands has a width equal to the resonance width. All distributions are fitted adequately. Figs. 14-18 show decay angular distributions for the same bands. Again, fits are acceptable. In this case, the decay angle α is with respect to the beam distribution after a Wick rotation. The definition and description of α are to be found in the Technical Report on data at 1350-1940 MeV/c.

7 Cross sections v. Momentum

Tables 4 and 5 collect together branching fractions and phases fitted to the data. At 900 MeV/c, I have evaluated errors by stepping the amplitude in

Channel		600	900	1050	1200	1350	1525	1642
$a_0(980)\eta$	$^1S_0$	7.2	10.8 ± 1.9	6.1	4.6	10.1	10.1	12.6
	$^3P_1$	3.5	0.0 ± 6.2	5.0	11.4	6.7	10.2	2.4
	$^1D_2$	0.4	3.5 ± 1.4	4.5	1.3	0.0	0.0	0.9
	$^3F_3$	-	4.5 ± 5.0	0.0	4.0	5.3	5.3	6.5
$f_0(1500)\pi$	$^1S_0$	39.6	7.4 ± 1.5	0.8	2.9	0.3	0.0	0.9
	$^3P_1$	4.9	5.6 ± 0.8	2.0	7.3	8.9	12.3	9.9
	$^1D_2$	1.3	7.5 ± 1.7	6.0	5.8	1.1	0.3	1.1
$a_2(1320)\eta$	$^1D_2\ L=0$	20.6	10.0 ± 3.5	12.2	5.4	6.0	4.6	1.2
	$^1D_2\ L=2$	-	1.4 ± 0.4	2.4	3.7	0.9	0.0	0.0
	$^1S_0$	-	0.8 ± 0.5	1.9	2.1	5.6	5.2	11.0
	$^3P_1$	2.2	5.3 ± 3.7	1.4	2.4	2.3	1.6	0.7
	$2^+\ m=0$	2.5	4.5 ± 1.1	7.8	8.6	8.7	9.2	5.0
	$^3F_3$	-	6.7 ± 3.2	4.3	6.9	5.3	0.0	0.0
	$2^+\ m=0, L=3$	-	4.3 ± 1.3	7.8	6.7	3.6	4.2	
$f_0(1750)\pi$	$^1S_0$	3.4	5.2 ± 0.5	11.2	9.3	1.5	0.1	5.1
	$^3P_1$	1.2	0.4 ± 0.7	0.6	0.8	0.0	2.7	1.8
$f_2(1525)\pi$	$^1D_2$	5.2	6.3 ± 2.7	2.9	-	-	-	-
	$^3P_1$	2.0	4.0 ± 0.8	4.4	-	-	-	-
$f_2(1270)\pi$	$^1D_2$	2.1	5.3 ± 0.5	3.2	3.5	5.6	5.9	6.0
$f_2(1980)\pi$	$^1D_2$	5.2	4.8 ± 1.5	3.3	2.0	3.4	2.3	0.7
	$^3P_1$	1.7	4.8 ± 3.8	2.3	2.9	2.9	4.8	4.4
	$2^+\ m=0$	-	4.6 ± 1.3	0.4	4.1	0.3	0.2	0.0
	$2^+\ m=1$	-	3.8 ± 2.2	2.2	7.9	7.7	9.5	6.9
	$^3F_3$	-	2.5 ± 1.4	4.1	0.9	6.1	6.0	8.2
$a_2(1660)\eta$	$^1D_2$	-	-	1.5	1.7	5.7	7.4	8.5

Table 4
Branching fractions (%) for individual partial waves v. beam momentum (MeV/c)

Channel		600	900	1050	1200	1350	1525	1642
$a_0(980)\eta$	$^1S_0$	-105	-140 ± 9	-144	-171	-177	-154	-149
	$^3P_1$	0	0	1	25	41	41	20
	$^1D_2$	-	-72 ± 7	-78	-90	-	-	-
	$^3F_3$	-	-	-	179	-170	-152	-165
$f_0(1500)\pi$	$^1S_0$	56	43	-	133	-	-	45
	$^3P_1$	0	0	0	0	0	0	0
	$^1D_2$	108	102 ± 8	99	84	101	-	114
$a_2(1320)\eta$	$^1D_2$ $L=0$	0	0	0	0	0	0	0
	$^1D_2$ $L=2$	-	-62 ± 45	-76	-72	-	-	-
	$^1S_0$	-	-90 ± 21	-90	-100	-91	-90	-65
	$^3P_1$	-70	-71	-72	-62	-55	-63	-
	2^+ $m=0$	0	0	0	0	0	0	0
	$^3F_3$	-	-109 ± 21	-85	-85	-81	-	-
	2^+ $m=0, L=3$	-	-	109	81	93	101	95
$f_0(1750)\pi$	$^1S_0$	-79	-67 ± 27	-95	-99	-115	-	8
	$^3P_1$	-90	-90 ± 35	-	-	-	-20	-6
$f_2(1525)\pi$	$^1D_2$	-27	-16 ± 15	-44	-	-	-	-
	$^3P_1$	19	21 ± 36	46	-	-	-	-
$f_2(1270)\pi$	$^1D_2$	-	126 ± 8	-	-	125	114	142
$f_2(1980)\pi$	$^1D_2$	-138	-107 ± 17	-143	-142	-135	-104	-90
	$^3P_1$	120	127 ± 35	138	99	122	144	112
	2^+ $m=0$	-	-59 ± 31	-	-63	-51	-61	-74
	2^+ $m=1$	-	16 ± 12	43	28	43	53	73
	$^3F_3$	-	-90 ± 35	-67	-	-90	-67	-88
$a_2(1660)\eta$	$^1D_2$	-	-	125	110	102	134	108

Table 5
Phases for individual partial waves v. beam momentum (MeV/c); a dash indicates that the amplitude is too small for a meaningful determination of the phase

magnitude or phase until log likelihood increases by 0.5. Branching fractions below 1% are unreliable, and for these cases I omit the phases from Table 5. A warning is that there is everywhere significant cross-talk between $L = 0$ and $L = 2$ and between $L = 1$ and $L = 3$. At some momenta, alternative solutions are to be found with similar log likelihood to the one I have accepted. However, these alternatives tend to generate several wildly different phases. Therefore, demanding that phases are tolerably smooth v. momentum has proved to be a way of rejecting alternative solutions. For singlet partial waves I adopt as reference phase that of $a_2(1320)\eta\ ^1D_2$ with $L = 0$, since it is large at most momenta. At 1642 MeV/c, where it is small, I take a suitable average of other large amplitudes. For triplet waves with $m = 1$, I use $f_0(1500)\pi\ ^3P_1$ as reference. For $m = 0$ triplet states, I use $2^+\ a_2(1320)\eta$ as reference.

Fig. 19(a) shows the integrated cross section for all $\eta\eta\pi^0$ events. The normalisation has been obtained from scaler readings of beam counts, corrected for deadtime within the data-recording system, and using event numbers corrected by the acceptance found by the Monte Carlo. A full account of this procedure will be given in the report on $\pi^0\pi^0$ final states.

Figs. 19(b)–(c) show cross sections for $\bar{p}p$ partial waves with quantum numbers 0^-, 2^-, 1^+, 2^+ and 3^+. The only distinctive feature of these figures is a strong rise of $0^- \to f_0(1500)\pi^0$ at 600 MeV/c. This is clearly visible from the strength of the $f_0(1500)$ band on the Dalitz plot of Fig. 1. (There is also a rise for 1^+, but this is distributed over many channels and is much smaller in magnitude). It is possible that this steep increase at low momenum for 0^- is due to the high mass tail of the VES $\pi(1800)$ [1], which they claim to be a hybrid. Decays to $f_0(1500)\pi$ are plausible for a hybrid. Remember too that the $f_0(1500)$ is quite strong in $\bar{p}p$ annihilation at rest; there, the branching ratio between $\eta\eta\pi^0$ and $\eta\pi^0\pi^0$ final states is 1/3, compared with the average 1/12 observed in flight by Bing Song and myself.

8 Earlier observations of $f_0(1770)$ and Interpretation

There has been extensive previous evidence for $f_0(1770)$, but most of it somewhat less definitive than the present data. A peak has been observed for $J = 0$ in two sets of data on $\pi^-\pi^+ \to K_sK_s$ [2,3]. Secondly, a partial wave analysis of $J/\Psi \to \gamma(4\pi)$ has fitted 4π peaks at this mass with $J = 0$ [4]. The GAMS group has reported [5] an $X(1740)$ decaying to $\eta\eta$ at 1744 ± 15 MeV, but they find a width < 90 MeV. Their angular distribution is flat, but spin 0 is not claimed because of uncertainty about the production mechanism. E760 MeV data [6] on $\bar{p}p \to \eta\eta\pi^0$ show peaks at 1500, 1748 ± 10 and 2100 MeV; they do not report a spin-parity analysis. In view of the fact that we observe strong production of $f_0(1500)$ and $f_0(2100)$ in our $\eta\eta\pi^0$ data, it seems plausible that

their peak at 1750 MeV may be the same resonance as we observe. Their width of 264 ± 25 MeV is acceptably close to ours. The BES group claims an f_0 at 1781 MeV in $J/\Psi \to \gamma(K^+K^-)$ [7].

Two 0^+ $q\bar{q}$ resonances are to be expected in this mass range. One is the radial excitation of $f_0(1300-1380)$. The second is the missing $s\bar{s}$ state from a 0^+ nonet made up of $f_0(1300-1380)$, $a_0(1450)$ and $K^*(1430)$. The resonance we observe could be either of these or a linear combination. The L3 group [8] has reported a narrow signal at 1793 ± 18 MeV in K_SK_S, but without a spin-parity determination. It is reported as having a very narrow width: 51 ± 19 MeV. Such a narrow width is incompatible with what we observe for $f_0(1770)$, as is clear from Fig. 6(d).

9 Acknowledgements

I wish to thank Bing Song Zou for extensive discussions and help and also say a big thank you to Andrei Sarantsev for the huge amount of work he has put into producing the data.

References

[1] D. Amelin et al., Phys. Lett. B356 (1995) 595 and (1996) 1021.

[2] B.V. Bolonkin et al., Nucl. Phys. B309 (1988) 426.

[3] A. Etkin et al., Phys. Rev. D25 (1982) 1786 and 2446.

[4] D.V. Bugg et al., Phys. Lett. B353 (1995) 378.

[5] D.Alde et al., Phys. Rev. B284 (1992) 457.

[6] T.A. Armstrong et al., Phys. Lett. B307 (1993) 394.

[7] J.Z. Bai et al., Phys. Rev. Lett. 77 (1996) 3959.

[8] M.Acciarri et al., Phys. Lett. B363 (1995) 118.

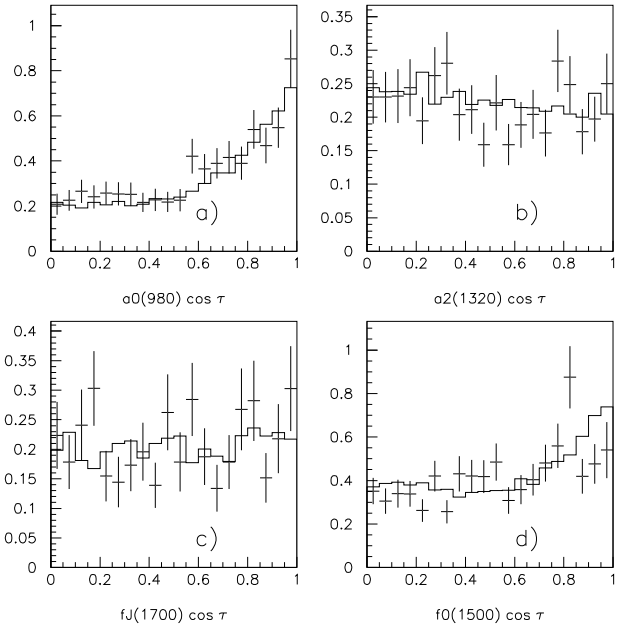

Fig. 9. Production angular distributions compared with the fit at 600 MeV/c; (a) a 65 MeV wide band around $a_0(980)$, (b) a 118 MeV wide band around $a_2(1320)$, (c) an $\eta\eta$ band from 1640 to 1840, (d) a 120 MeV wide band around $f_0(1500)$.

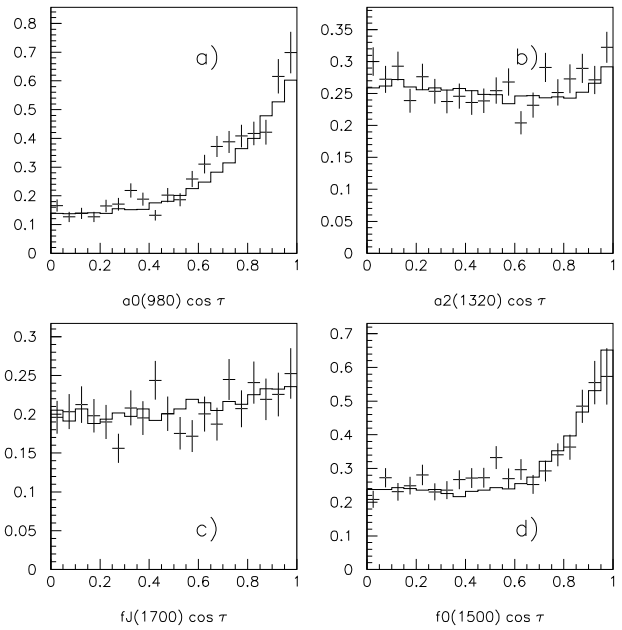

Fig. 10. As Fig. 9 at 900 MeV/c

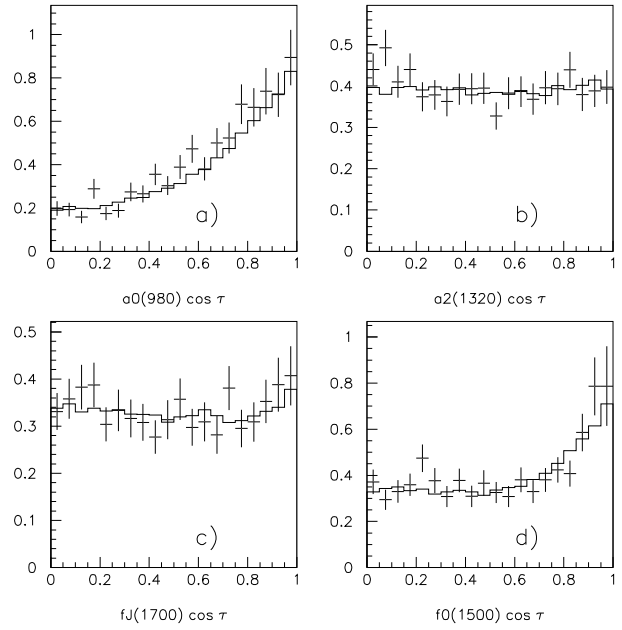

Fig. 11. As Fig. 9 at 1050 MeV/c

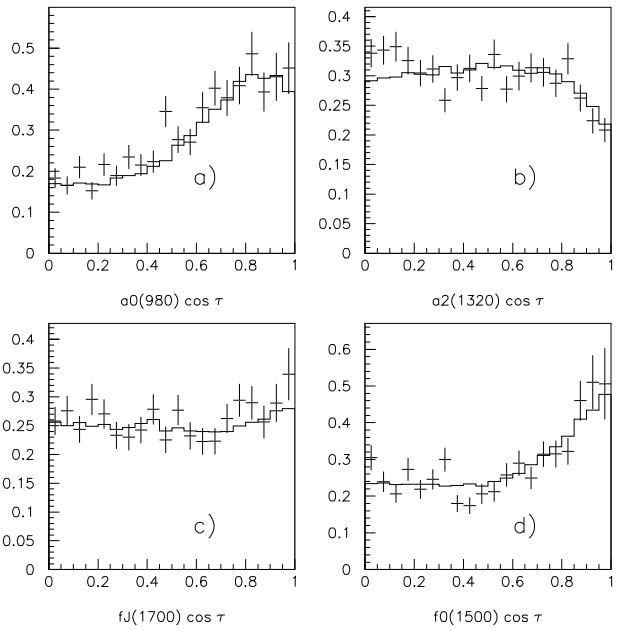

Fig. 12. As Fig. 9 at 1200 MeV/c

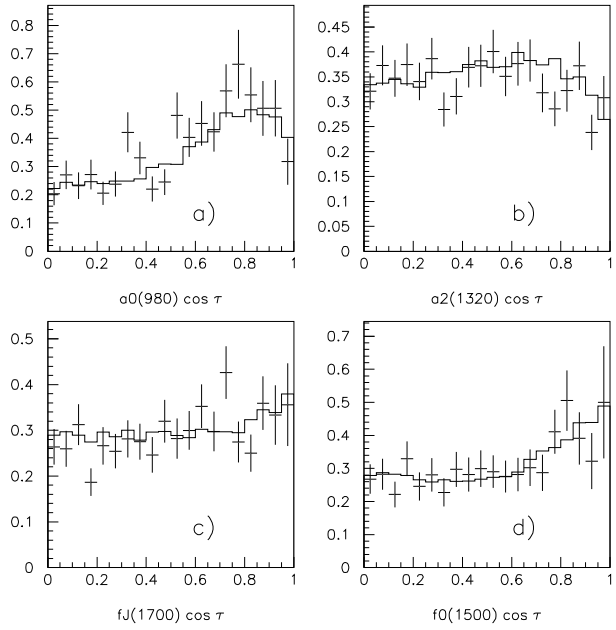

Fig. 13. As Fig. 9 at 1350 MeV/c

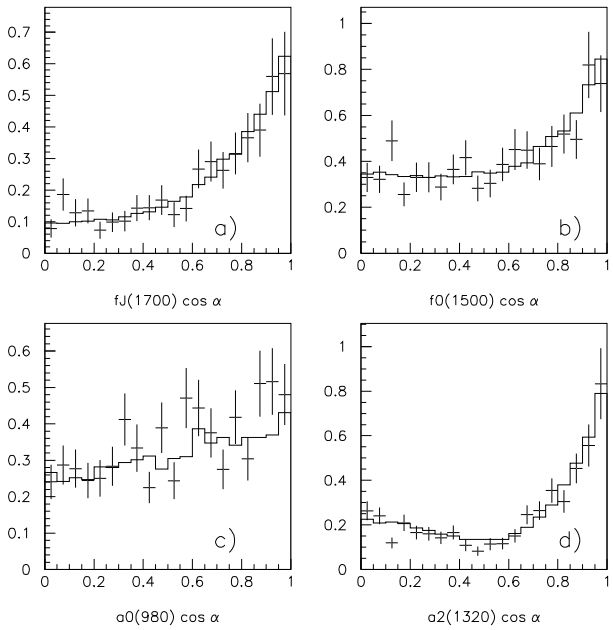

Fig. 14. As Fig. 9 for decay angular distributions at 600 MeV/c

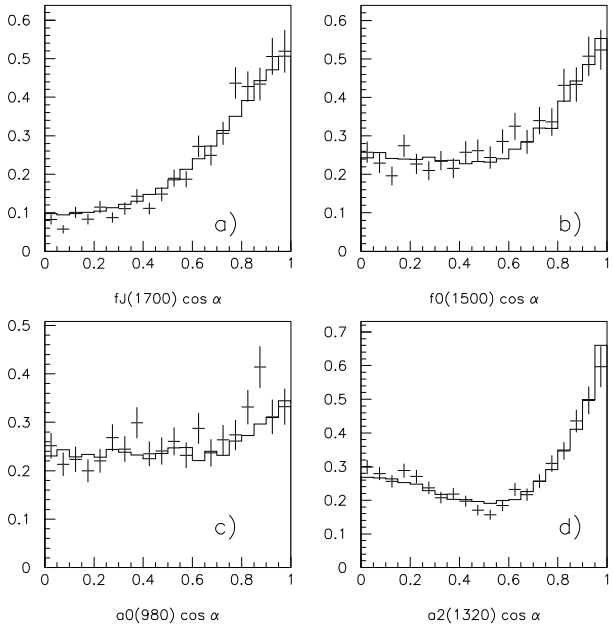

Fig. 15. As Fig. 14 at 900 MeV/c

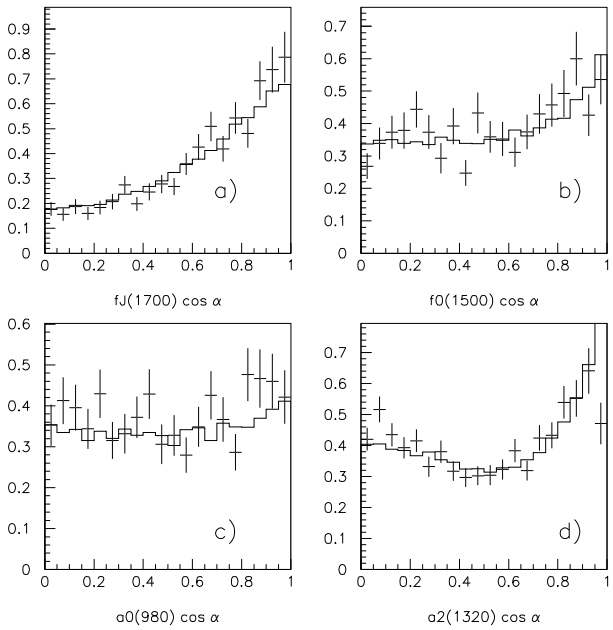

Fig. 16. As Fig. 14 at 1050 MeV/c

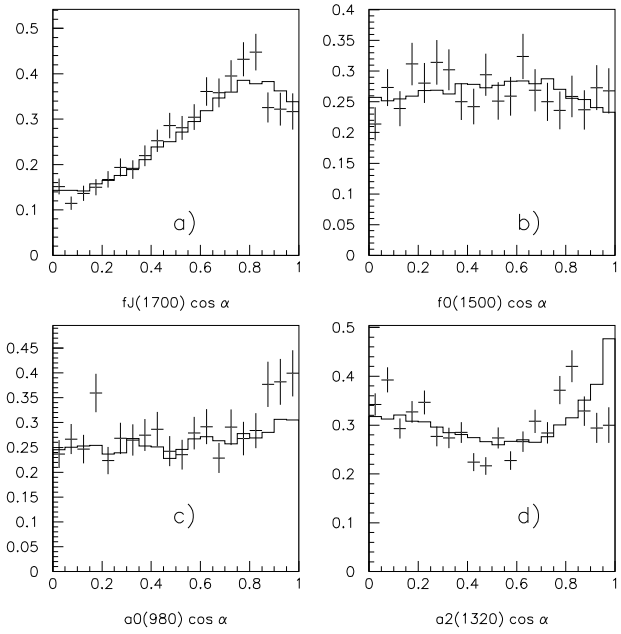

Fig. 17. As Fig. 14 at 1200 MeV/c

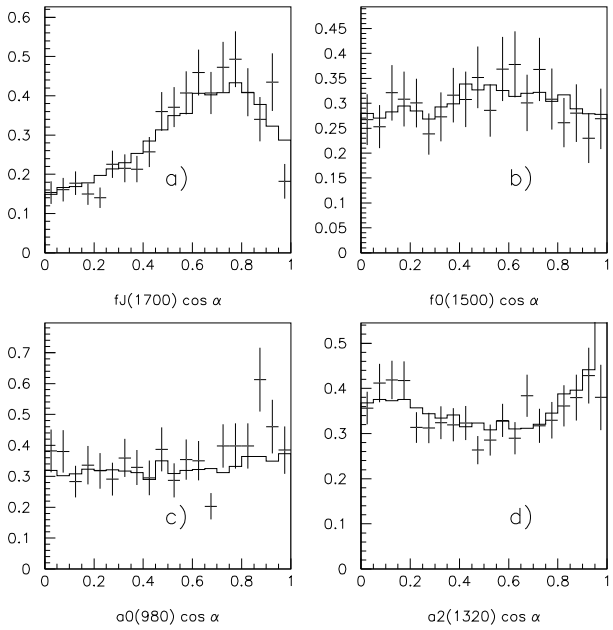

Fig. 18. As Fig. 14 for 1350 MeV/c.

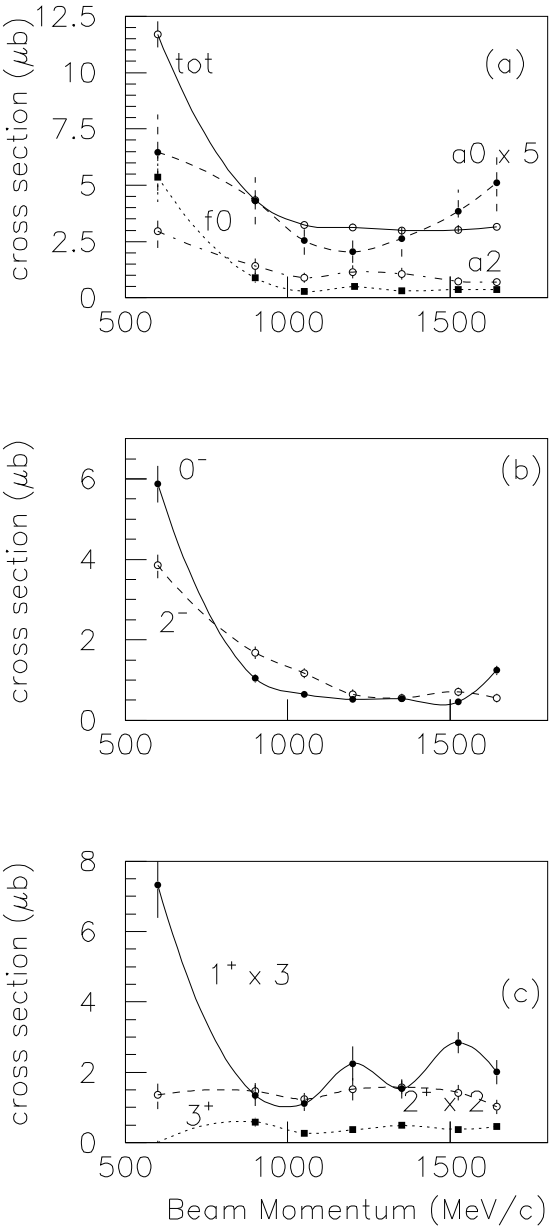

Fig. 19. Cross sections v. beam momentum for (a) all events (full curve), $f_0(1500)$(dotted), $a_0(980)$ (dashed) and $a_2(1320)$ (chain curve), (b) the summed 0^- and 2^- partial waves, (c) summed 1^+, 2^+ and 3^+ partial waves.